



An evaluation of the general composition and critical raw material content of bauxite residue in a storage area over a twelve-year period

Title	An evaluation of the general composition and critical raw material content of bauxite residue in a storage area over a twelve-year period
Author(s)	Cusack, Patricia B.; Courtney, Ronan; Healy, Mark G.; O'Donoghue, Lisa M. T.; Ujaczki, Éva
Publication Date	2018-10-09
Publisher	Elsevier
Repository DOI	10.1016/j.jclepro.2018.10.083

1 *Published as: Cusack, P.B., Courtney, R., Healy, M.G., O' Donoghue, L.T., Ujaczki, É. 2019. An*
2 *evaluation of the general composition and critical raw material content of bauxite residue in a storage*
3 *area over a twelve-year period. Journal of Cleaner Production 208: 393-401.*
4 <https://doi.org/10.1016/j.jclepro.2018.10.083>
5
6

7 An evaluation of the general composition and critical raw material content of bauxite residue
8 in a storage area over a twelve-year period
9

10 Patricia B. Cusack^{a,b}, Ronan Courtney^{a,b}, Mark G. Healy^c, Lisa M. T. O' Donoghue^d, Éva
11 Ujaczki^{b,d,e*}
12

13 ^aDepartment of Biological Sciences, University of Limerick, Castletroy, Co. Limerick, Ireland.

14 ^bThe Bernal Institute, University of Limerick, Castletroy, Co. Limerick, Ireland.

15 ^cCivil Engineering, National University of Ireland, Galway, Ireland.

16 ^dSchool of Engineering, University of Limerick, Castletroy, Co. Limerick, Ireland.

17 ^eDepartment of Applied Biotechnology and Food Science, Faculty of Chemical Technology
18 and Biotechnology, Budapest University of Technology and Economics, Műegyetem rkp. 3,
19 1111 Budapest, Hungary.
20

21 *Corresponding Author: Éva Ujaczki

22 E-mail address: eva.ujaczki@ul.ie
23

24 **Highlights**

- 25 • The composition of stored bauxite residue was examined in a residue disposal area.
- 26 • Bauxite residue critical raw material content did not vary over time in storage.
- 27 • The pH of the bauxite residue in storage ranged from 10 ± 0.1 to 12.0 ± 0.02 .
- 28 • The gallium content measured in the bauxite residue was $107 \pm 7.3 \text{ mg kg}^{-1}$.
29

30 **Abstract**

31

32 Bauxite residue, the by-product produced in the alumina industry, is being
33 produced at an estimated global rate of approximately 150 million tonnes per annum.
34 Currently, the reuse of bauxite residue is low (~ 2%), due to limitations associated with its
35 alkalinity, salinity, low solid content, fine particle size and potential leaching of metal(loid)s.
36 It has been identified as a potential secondary source for critical raw materials such as
37 vanadium, gallium and scandium, which currently have an associated supply risk and high
38 economic cost within Europe. However, there is an uncertainty regarding the possible
39 variation in these and other physico-chemical, elemental and mineralogical parameters
40 within bauxite residue disposal areas. This paper aimed to address this knowledge gap by
41 examining the variation of these parameters in a bauxite residue disposal area (BRDA) over a
42 twelve-year period. The general composition did not vary greatly within the bauxite residue
43 examined, with the exception of pH and electrical conductivity, which ranged from 10 ± 0.1
44 to 12.0 ± 0.02 and from 0.4 ± 0.01 to $3.3 \pm 0.2 \text{ mS cm}^{-1}$, respectively. The bauxite residue
45 contained critical raw materials, of which the amount of vanadium, gallium and scandium did
46 not vary significantly over time. The vanadium and gallium were present in larger amounts
47 compared to other European bauxite residues. On average the vanadium, gallium and
48 scandium content measured in the bauxite residue samples were 510 ± 77.8 , 107 ± 7.3 and
49 $51.4 \pm 5.4 \text{ mg kg}^{-1}$, respectively. This shows promise for the potential reuse of bauxite
50 residue as a secondary source for critical raw materials and also indicates that BRDAs may
51 be potential mines for critical raw material extraction.

52

53 **Keywords:** bauxite residue, bauxite residue disposal area, reuse value, critical raw materials

54

55 **Nomenclature**

56

57 Al aluminium

58 AlO(OH) boehmite

59 Al(OH)₃ aluminium hydroxide hydrate

60 Al₂O₃ aluminium oxide

61 As arsenic

62 BRDA(s) bauxite residue disposal area(s)

63 Bt billion tonnes

64 CaO calcium oxide

65 Ca(OH)₂ slaked lime

66 CaTiO₃ perovskite

67 Cd cadmium

68 Ce cerium

69 Co cobalt

70 CO₂ carbon dioxide

71 CRM(s) critical raw material(s) (mg kg⁻¹)

72 Cr chromium

73 Cu copper

74 DSC differential scanning calorimetry (mW)

75 Dy dysprosium

76 EC electrical conductivity (mS cm⁻¹)

77 EDS energy-dispersive x-ray spectroscopy (weight %)

78 Er erbium

79 Eu europium

80	EU	European Union
81	Fe	iron
82	FeO(OH)	goethite
83	Fe ₂ O ₃	iron oxide
84	Ga	gallium
85	Gd	gadolinium
86	HCl	hydrochloric acid
87	HNO ₃	nitric acid
88	Ho	holmium
89	ICP-OES	inductively coupled plasma optical emission spectrometer
90	In	indium
91	K α	k alpha
92	kV	kilovolt
93	La	lanthanum
94	Lu	lutetium
95	1M	1 molar
96	mA	milliamp
97	Mo	molybdenum
98	MPa	megapascal
99	Mt	million tonnes
100	N	nitrogen
101	NaOH	sodium hydroxide
102	Nd	neodymium
103	Ni	nickel
104	P	phosphorus

105	ρ_b	bulk density (g cm^{-3})
106	PGM	platinum group metals
107	PVDF	polyvinylidene difluoride
108	pH	pH (pH unit)
109	Pr	praseodymium
110	PSA	particle size analysis (μm and in % of the total particle distribution)
111	REE(s)	rare earth element(s) (mg kg^{-1})
112	REO(s)	rare earth oxide(s)
113	Sc	scandium
114	SEM	scanning electron microscope (μm)
115	SiO_2	silicon oxide
116	Sm	samarium
117	Tb	terbium
118	TGA	thermogravimetric analysis (mg)
119	Ti	titanium
120	TiO_2	titanium oxide
121	Tm	thulium
122	Tn	terbium
123	V	vanadium
124	XRD	x-ray diffraction ($^{\circ}2\Theta$)
125	XRF	x-ray fluorescence (%)
126	Y	yttrium
127	Yb	ytterbium
128		
129		

130 **1. Introduction**

131

132 Bauxite residue (red mud) is the by-product generated during the extraction of alumina from
133 bauxite ore using the Bayer Process (Kirwan *et al.* 2013), and is currently being produced at a
134 global rate of 150 Mt per annum, adding to the 3 Bt already in storage worldwide (Evans
135 2016). Currently, less than 2 % of the bauxite residue generated annually is being reused
136 (Ujaczki *et al.* 2018), with the remaining ~ 98 % going into bauxite residue disposal areas
137 (BRDAs) (Burke *et al.* 2013). The average cost of disposing and managing of bauxite
138 residue in storage is 1-2 % of the alumina price for the alumina refinery (Tsakiridis *et al.*
139 2004).

140

141 Current best practice guidelines for the storage of bauxite residue is to use dry-stacking, a
142 method which involves the thickening of the bauxite residue slurry from the Bayer process,
143 using a filter press or vacuum filtration (depending on the refinery), before being spread in
144 layers in the BRDA (Power *et al.* 2011; Evans 2016). Depending on the nature of the bauxite
145 ore used, some refineries operate a separation technique (Evans 2016), which allows the
146 bauxite residue to be separated into two main size fractions: a fine fraction (particle size <100
147 μm) and a coarse fraction (particle size > 150 μm) (IAI 2015; Jones *et al.* 2012). Bauxite
148 residue is typically characterised as being highly alkaline, saline and composed of mainly fine
149 particles comprised of a wide range of metal(loid)s and minerals (Gräfe *et al.* 2009). This
150 poses challenges in the long-term management of BRDAs in terms of protecting the
151 surrounding environment (Higgins *et al.* 2017; Kong *et al.* 2017), due to the high alkalinity,
152 increased risk of dust pollution (due to the fine particles), and leaching of trace elements
153 (Wang *et al.* 2015; Kong *et al.* 2017). The disposal conditions and management of residue in
154 a BRDA is dependent on many factors such as location, climate, engagement with local

155 communities and stakeholders (IAI 2015) and involves licencing permits from regulatory
156 authorities (such as the Environmental Protection Agency). For example, European operators
157 must meet the requirements according to the European List of Waste and Directive (EU
158 Communities 1999, 2002). As a result of this, some refineries implement neutralisation
159 techniques prior to disposal, such as carbon dioxide (CO₂) sparging of residues (Cooling
160 2007) or post disposal through the use of atmospheric carbonation (mud farming) with
161 amphirolling (Evans 2016) in the BRDA, which helps in the neutralisation, dewatering and
162 compaction of the bauxite residue (Evans 2016; Gomes *et al.* 2016; Higgins *et al.* 2016; Zhu
163 *et al.* 2016), reducing both alkalinity and moisture content, which are two limitations to the
164 re-use of bauxite (Evans 2016).

165

166 Traditionally, the reuse of bauxite residue has focussed on construction applications such as
167 cementitious application (Pontikes and Angelopoulos 2013; Nikbin *et al.* 2018). Some other
168 reuse options for bauxite residue have included polymers (Hertel *et al.* 2016), ceramics
169 (Pontikes *et al.* 2009) and catalysts (Wang *et al.* 2008); adsorbents for wastewater treatment
170 (Bhatnagar *et al.* 2011), particularly for the removal of arsenic (As) (Arco-Lázaro *et al.*
171 2018), chromium (Cr) (Dursun *et al.* 2008), nickel (Ni) (Hannachi *et al.* 2010), copper (Cu)
172 (Atasoy and Bilgic 2018), cadmium (Cd) (Ha *et al.* 2017) and phosphorus (P) (Cusack *et al.*
173 2018), as well as applications as potential soil ameliorants (Ujaczki *et al.* 2015). More
174 recently and due to the demand of critical raw materials (CRMs), particularly the rare earth
175 elements (REEs), studies have examined the potential of bauxite residue as a secondary
176 source of these materials and their potential economic value (Gomes *et al.* 2016; Xue *et al.*
177 2016; Ujaczki *et al.* 2017).

178

179 Within the European Union (EU), the ‘Raw Materials Initiative’ ensures that Europe secures
180 and sustains an affordable supply of CRMs which are identified as being of high economic
181 importance and having a risk to their supply (EU COM/2017/0490). The list of 27 CRMs
182 features elemental groups and single elements, including platinum group metals (PGM) and
183 REEs (EU COM/2017/0490). The REEs are divided into light REE [lanthanum (La), cerium
184 (Ce), praseodymium (Pr), neodymium (Nd), samarium (Sm), europium (Eu)] and heavy REE
185 [gadolinium (Gd), terbium (Tb), dysprosium (Dy), holmium (Ho), erbium (Er), thulium
186 (Tm), ytterbium (Yb), lutetium (Lu), including yttrium (Y)] (Xu *et al.* 2017) plus scandium
187 (Sc) (Binnemans *et al.* 2018). Depending on the origin of the bauxite residue generated, it
188 may be a potentially valuable source of CRM and other elements e.g. REEs, Sc, V, Ga, and
189 titanium (Ti) (Liu and Naidu 2014). Also included in the 2017 CRM list is P and phosphate
190 rock, which are also of particular interest, as bauxite residue has been previously identified as
191 having a high P retention capacity (Grace *et al.* 2015, 2016; Cusack *et al.* 2018) due to its
192 high aluminium (Al) and iron (Fe) oxide content (IAI 2015), making it a possible resource in
193 the removal and recovery of P from aqueous solutions (Grace *et al.* 2015; Cusack *et al.*
194 2018).

195

196 Although bauxite residues are typically similar in composition, properties can vary between
197 refineries and this is attributed to the type of ore used, as well as different process parameters,
198 such as temperature, pressure and concentrations of caustic soda (NaOH), slaked lime
199 (Ca(OH)₂) and other additives used in the Bayer process (Gräfe *et al.* 2009; Gräfe *et al.*
200 2011). This indicates that re-use options should be refinery-specific (Balomenos *et al.* 2017).
201 A further potential limitation, is that bauxite residue composition, such as pH and bulk
202 density, may change over time in storage (Kong *et al.* 2017a; Zhu *et al.* (2016a,b), which
203 greatly influences the possibility of reusing bauxite residue.

204

205 To date, no study has investigated the CRM content variability in bauxite residue stored
206 within one specific BRDA. Therefore, the objectives of this study were to: (1) characterise
207 the physico-chemical, elemental and mineralogical composition of the dominant fraction
208 (fine fraction) bauxite residue in storage over a twelve-year period, and to determine if there
209 is any variation over the time spent in storage, which could affect possible reuse of the
210 bauxite residue (2) create an inventory of economically interesting elements in bauxite
211 residue over the storage period, and (3) calculate the financial value of economically
212 interesting elements present in the bauxite residue.

213

214 **2. Materials and Methods**

215

216 2.1 Site description and sample collection

217 Bauxite residue was obtained from a European refinery, who operated a separation technique
218 to isolate the fine (particle sizes <100 µm) and coarse (particle sizes >150 µm) fractions of
219 bauxite residue before disposal (IAI 2015), in an approximate ratio of 9:1 (fine: coarse).

220 Bauxite residue was sampled to a depth of 30 cm and the bulk samples were stored in 1 L
221 containers, returned to the laboratory, and dried at 105°C for 24 hr. Once dry, the samples
222 were pulverised using a mortar and pestle and sieved to a particle size < 2 mm. In this paper,
223 the age of the samples will be described (Table 1) relative to the sample collection time
224 (2016).

225 2.2 Characterisation Study

226 2.2.1 Physico-chemical composition

227 The bauxite residue samples were characterised (n=3) for their physical, chemical, elemental
228 and mineralogical properties (Figure 1). The pH and electrical conductivity (EC) were
229 measured using a 5 g sample in an aqueous extract, using a 1:5 ratio (solid: liquid) (Courtney
230 and Harrington, 2010). The bulk density (ρ_b) was determined after Blake (1965), the
231 effective particle size analysis (PSA) was determined on particle sizes $< 53 \mu\text{m}$ using optical
232 laser diffraction on a Malvern Zetasizer 3000HS® (Malvern, United Kingdom) with online
233 autotitrator and a Horiba LA-920, and reported at specific cumulative % (10, 50 and 90 %).
234 Thermogravimetric analysis (TGA) was carried out to identify any change in mass over time
235 with temperature, and change in heat flow over time with temperature was analysed using
236 differential scanning calorimetry (DSC). TGA and DSC were carried performed using a
237 Labsys TG (DSC/TGA 1600) in a nitrogen (N) atmosphere at a temperature range of 30 °C to
238 1000 °C at a heating rate of 10 °C min⁻¹ (Borra *et al.* 2015). Due to cost limitations, only six
239 samples were analysed (BR12, BR10, BR8, BR6, BR4 and BR2).

240

241 2.2.2 Mineralogical composition

242 Mineralogical detection was carried out on 1 g powdered samples using X-ray diffraction
243 (XRD) on a Philips X'Pert PRO MPD® (California, USA) at 40 kV, 40 mA, 25 °C by Cu X-
244 ray tube ($K\alpha$ -radiation). The patterns were collected in the angular range from 5 to 80 ° (2θ)
245 with a step-size of 0.008 ° (2θ) (Castaldi *et al.* 2011), whilst surface morphology and
246 elemental detection were carried out using scanning electron microscopy (SEM) and energy-
247 dispersive X-ray spectroscopy (EDS) on a Hitachi SU-70 (Berkshire, UK). X-ray
248 fluorescence (XRF) analysis was carried out onsite at the refinery using a Panalytical Axios
249 XRF (Malvern, UK).

250
251
252
253
254
255
256
257
258
259
260
261
262
263
264
265
266
267
268
269
270
271
272
273
274

2.2.3 Elemental composition

Chemical analysis of minor elements was performed after aqua regia digestion (HCl: HNO₃) with a solid to liquid ration of 1:10 in a Multiwave 3000 (Rotor 8XF100) type microwave digestion system at 200 °C 1.25 MPa. After digestion, the solutions were filtered through 0.45 µm PVDF syringe filters and diluted in 1 M HNO₃ for the analysis (Ujaczki *et al.* 2017). The metal analysis was carried out using an Agilent Technologies 5100 inductively coupled plasma optical emission spectrometer (ICP-OES). The calibration curve was constructed using standard solutions of 100, 50, 10, 5 and 1 g L⁻¹ multi-element standard (Inorganic Ventures, Ireland) and 5, 2.5, 0.5, 0.25 and 0.05 g L⁻¹ REE standard (Inorganic Ventures, Ireland). The 1M HNO₃ solution was also used for the dilutions of the standard solutions and as a calibration blank. For the ICP-OES analysis, the following analytical lines (in nm) were used for the calculations of each of the elements: Ce 418.659, 446.021; cobalt (Co) 228.615, 230.786; Dy 353.171; Er 349.910, 369.265; Eu 397.197, 412.972, 420.504; Ga 294.363; Gd 335.048, 336.224; Ho 339.895, 345.600, 389.094; indium (In) 230.606, 352.609; La 333.749, 379.477, 408.671; Lu 261.541, 307.760; molybdenum (Mo) 202.032, 203.846, 204.598; Nd 401.224, 406.108, 410.945; Pr 390.843, 417.939; Sc 335.372, 361.383, 363.074; Sm 359.259, 360.949; Tb 350.914,367.636; Tm 313.125, 342.508; Y 360.074, 371.029, 377.433; Yb 289.138, 328.937, 369.419; V 268.796, 292.401, 311.070 (Bridger and Knowles, 2000).

2.3 Statistical Analysis

Pearson’s correlation coefficients were used to determine any relationships between age of sample and sample properties (pH, EC, bulk density, particle size, mineralogical composition and elemental composition), using IBM SPSS Statistics 24.

275 3. Results

276 3.1 Physico-chemical composition

277 The pH of the bauxite residue (Table 2) ranged from 10.0 ± 0.1 to 12.0 ± 0.02 over the
278 twelve-year period, with the ten-year-old sample (BR10) having the highest value. The EC
279 (Table 2) of the bauxite residue ranged from 0.4 ± 0.01 to $3.3 \pm 0.2 \text{ mS cm}^{-1}$, with again, the
280 highest being for BR10. Small variation in the moisture content (Table 2) for the each of the
281 bauxite residues was recorded. The bulk density (Table 2) for the bauxite residue ranged
282 from 1.2 ± 0.1 to $1.5 \pm 0.02 \text{ g cm}^{-3}$.

283
284 The bauxite residue had a high composition of fine particles, which ranged from 0.6 ± 0.01 to
285 $12.7 \pm 2.3 \text{ }\mu\text{m}$ (Table 2). There was some agglomerate formation evident in all samples, as
286 seen in the accumulation of finer particles in the images captured by SEM (Figure S1, S2, S3
287 in the Supplementary Information). The medium value, d_{50} , of the particle size distribution
288 for bauxite residues ranged from $2.2 \pm 0.1 \text{ }\mu\text{m}$ (BR1) to $4.3 \pm 0.4 \text{ }\mu\text{m}$ (BR9). Ninety percent
289 of the distribution (d_{90}) was under $12.7 \pm 2.7 \text{ }\mu\text{m}$ and 10 % (d_{10}) was under $0.5 \pm 0.01 \text{ }\mu\text{m}$
290 (Table 2). Iron, Al, sodium (Na), calcium (Ca), titanium (Ti), and silicon (Si) were the main
291 elements present in all the bauxite residue samples (Figure S4). TGA curves showed weight
292 loss between 300 and 975 °C for all the bauxite residues (Figures 2 and S5). However,
293 sample BR12 (from 2014) had a larger temperature range over which weight loss occurred
294 (between 150 and 975 °C).

295

296 3.1.1 Mineralogical Composition

297 The main mineralogical composition of the bauxite residue detected by XRD included
298 haematite (Fe_2O_3), goethite ($\text{FeO}(\text{OH})$), perovskite (CaTiO_3), rutile (TiO_2), gibbsite $\text{Al}(\text{OH})_3$,
299 sodalite ($\text{Na}_8(\text{Al}_6\text{Si}_6\text{O}_{24})\text{Cl}_2$) and cancrinite ($\text{Na}_6\text{Ca}_2(\text{CO}_3)$) (Figure S6 and S7). Sample BR9
300 had an extra rutile peak at position $27.459^\circ 2\theta$ and no sodalite peak at position $14^\circ 2\theta$;
301 samples BR1 to BR6 had similar patterns, but with less intense peaks and sodalite peaks at
302 position $14^\circ 2\theta$ (Figure S6). Sample BR1 had one peak of boehmite ($\text{AlO}(\text{OH})$) at position
303 $13.9^\circ 2\theta$ and gibbsite at position $18.5^\circ 2\theta$ (Figure S6). Sample BR1 also had an
304 unidentified peak at position $47^\circ 2\theta$ (Figure S6).

305

306 XRF analysis carried out on the bauxite residue samples (Table 3) reflected the main
307 mineralogical composition detected by XRD analysis. The dominant oxides found were
308 Fe_2O (ranging from 40.1 ± 1.40 to 47.5 ± 2.0 %) and Al_2O_3 (14.8 ± 1.5 to 17.8 ± 0.73 %).
309 SiO_2 (7.20 ± 1.0 to 10.9 ± 0.47 %), TiO_2 (8.62 ± 0.71 to 10.3 ± 0.95 %) and CaO (5.70 ± 0.66
310 to $6.1 \pm 1.0\%$) were also present (Table 3).

311

312 3.1.2 Elements of economic importance in bauxite residue

313 An extensive inventory of CRMs and further elements of economic importance were
314 developed using microwave-assisted aqua regia digestion, with subsequent ICP-OES analysis
315 (Table 4). Overall, no trend was noted in the elemental content between the oldest and
316 newest bauxite residue in the BRDA. However, In, Mo, Ce, Nd, Dy and Er were present in
317 smaller amounts in the oldest samples compared to the fresh sample. Terbium (Tb), Tm and
318 Ho were not detected in the bauxite residue.

319

320 **4. Discussion**

321 4.1 Characterisation of bauxite residue

322 Bauxite residue typically has a pH >10 (Goloran *et al.* 2013) and an EC ranging from 1.4 to
323 28.4 mS cm⁻¹ (Gräfe *et al.* 2011). The high pH is attributed to the presence of alkaline anions
324 such as hydroxides (OH⁻), carbonate or bicarbonates (CO₃²⁻ / HCO₃⁻), aluminates or
325 aluminium hydroxides (Al(OH)₄⁻ / Al(OH)₃), and di/trihydrogen orthosilicates (H₂SiO₄²⁻ /
326 H₃SiO₄⁻) introduced and formed during the Bayer process (Gräfe *et al.* 2011). At the end of
327 the Bayer process, prior to disposal, residue undergoes a repeated washing stage. However,
328 the bauxite residue remains highly alkaline due to the alkalinity being in the form of slow
329 dissolving solid phases (Gräfe *et al.* 2011).

330

331 Depending on the refinery and the advances in residue management steps employed, the pH
332 may be further reduced through practices such as atmospheric carbonation (mud farming)
333 (Clohessy 2015; Evans 2016), seawater disposal (Menziez *et al.* 2009), application of spent
334 acid (Kirwan *et al.* 2013), phosphogypsum (Xue *et al.* 2018), or by the addition of an acidic
335 gas such as CO₂ or SO₂ (Xue *et al.* 2016). Consequently, surface pH values for residues may
336 vary between refineries and within BRDAs.

337

338 The bauxite residue examined in this study showed variation in terms of both the pH and the
339 EC (p < 0.01) (Table 2). Whilst the pH and EC did decrease across all the bauxite residue
340 samples examined in this study (Table 2), this was attributed to different causes. The reduced
341 pH value of the fresh bauxite residue examined (BR1) in this study (Table 2) is as a result of
342 the atmospheric carbonation technique, mud farming, which can effectively decrease
343 alkalinity (Clohessy 2015; McMahon 2017). This helps in removing the alkalinity

344 limitation/barrier to the reutilisation of the bauxite residue (Evans 2016) and has been shown
345 to successfully decrease the pH of fresh bauxite residue (~ 13.5) to below < 11.5 within seven
346 days (Clohessy 2015). The mud farming technique sequesters CO₂ from the atmosphere,
347 allowing for the accelerated carbonation of the bauxite residue (IAI 2015; Evans 2016). Due
348 to this process, the free OH⁻ present in the bauxite residue is neutralised due to the
349 carbonation of the CO₂ present in the surrounding atmosphere (air), resulting in the formation
350 of carbonates, therefore creating a buffering effect, which results in a drop in pH (Han *et al.*
351 2017).

352

353 Natural weathering processes may play an important role in the improvement of the physico-
354 chemical composition of bauxite residue in storage (Zhu *et al.* 2018). The reduction observed
355 in the pH of the older samples (Table 2) is as a result of the natural ageing and weathering of
356 the bauxite residue in storage. Evidence of the natural weathering decreasing the pH was
357 shown by Khaitan *et al.* (2010), who reported a pH of 10.5 for 14-year-old bauxite residue
358 and 9.5 for 35-year-old bauxite residue, with the decreases attributed to the slow carbonation
359 from atmospheric CO₂. Zhu *et al.* (2016a,b) also measured a decrease in residue pH from
360 10.98 to 9.45 in stored bauxite residue exposed to natural weathering processes. Similar to
361 pH, EC usually decreases with time in the storage area due to weathering (Zhu *et al.* 2016a,b;
362 Kong *et al.* 2017a). Rainfall events allow the soluble alkaline minerals such as sodalite and
363 calcite, which result in a buffering effect for both pH and salinity (EC) (Santini and Fey,
364 2013).

365

366 The thermal analysis (TGA/DSC) indicated an overall weight loss occurring between 300 and
367 975 °C for all the bauxite residue samples examined. Previous work has shown weight loss
368 between temperature ranges of 300 and 600 °C (attributed to the decomposition of

369 hydroxides in different stages), 300 and 400 °C (as a result of the decomposition of diaspora),
370 and between 600 and 800 °C (due to the decomposition of calcium carbonate) (Agatzini-
371 Leonardou *et al.* 2008), all dominant minerals in bauxite residue. There were numerous
372 endothermic peaks observed on the DSC curve for the six samples examined, particularly in
373 the region above 800°C. Endothermic peaks above this temperature are indicative of the
374 decomposition of sodalite phases and also the decomposition of quartz, which occurs
375 between 550 to 1000°C (Atasoy 2005). Small endothermic peaks throughout the DSC curve
376 may be attributed to loss of physically held water (Atasoy, 2005), which was notable in all
377 the bauxite residue samples examined.

378

379 The mineralogical composition of bauxite residue typically comprises Al₂O₃ and Fe₂O₃ in the
380 range of 20 to 45 % and 10 to 22 %, respectively (IAI 2015). This composition is reflected in
381 the XRF and XRD analysis, which showed the dominant presence of Fe₂O₃, FeO(OH), and
382 Al(OH)₃. CaTiO₃, AlO(OH) and TiO₂ were also detected in all samples, which is common
383 amongst bauxite residue (Gräfe *et al.* 2011). Sodalite (Na₈(Al₆Si₆O₂₄)Cl₂) was also present in
384 the bauxite residue, and is one of the most common desilication products formed during the
385 pre-desilication stage during the Bayer process, along with CaTiO₃ which is often found as a
386 result of the lime added (Gräfe *et al.* 2011).

387

388 4.2 Economic value of bauxite and potential for reuse

389 In recent years, several studies have been conducted to investigate the potential use of
390 industrial residues such as phosphogypsum, mine tailings, slags and bauxite residue as a
391 possible source for CRMs and REEs (Binnemans *et al.* 2015). Currently, the global
392 production rate of REEs, which is typically expressed in tons of rare earth oxides (REOs) is
393 130,000 to 140,000 tons, of which 95% is produced in China (Binnemans *et al.* 2018). Five

394 of the REEs (Nd, Eu, Tb, Dy, Y) are now described as being of a high supply risk within
395 Europe, Japan and the USA (Binnemans *et al.* 2018). Such CRMs and REEs are necessary
396 for the production of magnets, lighting, lasers, batteries, catalysts, and alloys in aerospace
397 (Weng *et al.* 2015).

398

399 While this study did show differences in the bauxite residue over the twelve-year period, in
400 terms of decreased pH and EC, there were no significant changes in the CRM content of the
401 bauxite residue (Table 4). This indicates that some BRDAs may be a potential resource for
402 the reprocessing and recovery of CRMs and REEs. However, this is not certain for all
403 BRDAs, as variation can and does occur within BRDAs and refineries due to differences in
404 bauxite ore type, parameters used within the Bayer Process, as well as varying disposal and
405 neutralisation techniques.

406

407 The Sc, Ga and V content of the bauxite residue in the current study are of particular interest,
408 due to their high economic value (Table 5) and supply risk. Scandium, a trace constituent of
409 igneous rocks (European Commission, 2017), is used in the production of aluminium alloys
410 (Ricketts and Duyvesteyn 2018), and V, present in minor amounts in the Earth's crust and
411 seawater and the majority of which is sourced as a by-product of the steel industry (European
412 Commission, 2017), is used in electrodes (Morel *et al.* 2016). Gallium is primarily sourced
413 from bauxite ore and bauxite residue, as it found naturally as a trace element dispersed in
414 minerals, which also includes coal (Qin *et al.* 2015), and is used in the production of catalysts
415 (Qin and Schneider 2016). The Sc in this study (Table 4) was lower than values found in
416 fresh Hungarian (Ujaczki *et al.* 2017), Greek (Borra *et al.* 2015), Russian (Petrakova *et al.*
417 2015) and Australian (Wang *et al.* 2013) bauxite residues. However, the Ga content (Table
418 4) was higher than that found by Ujaczki *et al.* (2017) in Hungarian bauxite residue, as well

419 as in Australian (Wang *et al.* 2013), Indian (Mohapatra *et al.* 2012) and Turkish
420 (Abdulvaliyev *et al.* 2015) bauxite residues. Finally, the V content was present in higher
421 amounts compared to Hungarian (Ujaczki *et al.* 2017), Indian (Mohapatra *et al.* 2012) and
422 Turkish (Abdulvaliyev *et al.* 2015) bauxite residues. This is indicative of the variation of
423 CRM content in residues between refineries. In addition to Sc, Ga and V, there is now a
424 focus on further valuable element extraction (Jowitt *et al.* 2018) and recovery of REE due to
425 the overproduction of REEs such as La and Ce, which is leading to an imbalance in the
426 supply of REEs produced and a demand for Nd and Dy (Binnemans and Jones 2015;
427 Binnemans *et al.* 2018), both of which were found in the bauxite residue in this study.

428

429 The typical methods of CRM recovery from bauxite residue include direct leaching using
430 mineral acids such as HNO₃, sulphuric acid (H₂SO₄) or hydrochloric acid (HCl), or leaching
431 following pyrometallurgical applications such as roasting (Ujaczki *et al.* 2018). Although
432 there are high recovery rates of CRMs from bauxite residue reported (Abdulvaliyev *et al.*
433 2015; Borra *et al.* 2015), so too are the associated costs for acids and energy required in these
434 processes, which questions the justification of extracting CRMs from by-products such as
435 bauxite residue. Recent studies have also highlighted the need to develop new technologies
436 to optimise the efficiency of CRM recovery from bauxite residue to ensure cost-effectiveness
437 (Gomes *et al.* 2016; Akcil *et al.* 2017). Ujaczki *et al.* (2018) in their review on the reuse of
438 bauxite residue as a source of CRMs, highlighted the extent of the benefits following CRM
439 recovery from a wider perspective in terms of the technological (development of more
440 efficient technologies), social (such as improvements to health), economic (mainly reduction
441 in refinery disposal costs), and environmental factors such as reduced emissions and loss of
442 habitable land.

443

444 4.3 The findings of this study from an industrial perspective on potential re-use of bauxite
445 residue
446 This study found that there was very little variation in the CRM content of bauxite residue in
447 a BRDA over a twelve-year period. This shows promise for the potential reuse of bauxite
448 residue as a secondary source of CRMs. Finding a suitable and long-term use for bauxite
449 residue may be hampered by several barriers and limitations (Klauber *et al.* 2011; Evans
450 2016), such as high alkalinity and salinity which were shown by this study to be reduced by
451 weathering and mud farming. However, limitations to the reuse of bauxite residue may be
452 overcome through management strategies involving its partial neutralisation and increased
453 solids content (Klauber *et al.* 2011).

454

455 **5. Conclusions**

456 This study showed that there was a reduction in both the pH and the EC ($p < 0.01$) of bauxite
457 residue in a BRDA over a twelve-year period. There was little variation in the CRM content
458 of the bauxite residue sampled. The CRMs of particular interest were V, Ga and Sc due their
459 potential supply risk and associated economic value. The V, Ga and Sc content of the bauxite
460 residue samples were 510 ± 77.8 , 107 ± 7.3 and 51.4 ± 5.4 mg kg⁻¹, respectively, giving
461 current economic values of 3.51, 42.73 and 236.44 US \$ t⁻¹. From a European and global
462 context, this highlights a potential resource for CRMs in the event of a scarcity of these
463 materials. However, the general composition and CRM content of bauxite residue varies
464 greatly due to the bauxite ore and parameters used in the Bayer Process, as well as the
465 disposal and neutralisation methods implemented by refineries. Depending on the history of
466 the refinery and BRDA, there may be little variation over time, making BRDAs possible
467 sources for the extraction of CRMs. There are currently high-costs associated with the
468 extraction of CRMs from bauxite residue due to the large amount of reagent and/or energy

469 required in the process, before purifying the CRMs recovered for reuse. However, these need
470 to be set against the overall benefits of recovering CRMs in terms of the environmental,
471 economic and social factors. Further research is necessary to investigate the cost and
472 environmental implications and limitations of extraction of CRMs from BRDAs, as opposed
473 to conventional extraction techniques from mines, in terms of emissions produced, machinery
474 required, fuel needed and human resources required.

475

476 **Acknowledgements**

477 The authors would like to acknowledge the financial support of the Environmental Protection
478 Agency (EPA) (2014-RE-MS-1).

479

480 **References**

481 Abdulvaliyev, R.A., Akcil, A., Gladyshev, S.V., Tastanov, E.A., Beisembekova, K.O.,
482 Akhmadiyeva, N.K. and Deveci, H., 2015. Gallium and vanadium extraction from red mud of
483 Turkish alumina refinery plant: Hydrogarnet process. *Hydrometallurgy* 157, 72-77.

484

485 Agatzini-Leonardou, S., Oustadakis, P., Tsakiridis, P.E. and Markopoulos, C., 2008. Titanium
486 leaching from red mud by diluted sulfuric acid at atmospheric pressure. *J. Hazard. Mater.* 157,
487 579-586.

488

489 Akcil, A., Akhmadiyeva, N., Abdulvaliyev, R., Abhilash and Meshram, P., 2018. Overview on
490 extraction and separation of rare earth elements from red mud: focus on scandium. *Mineral.*
491 *Process. Extract. Metall. Rev.* 39,145-151.

492

493 Arco-Lázaro, E., Pardo, T., Clemente, R. and Bernal, M.P., 2018. Arsenic adsorption and plant
494 availability in an agricultural soil irrigated with As-rich water: effects of Fe-rich amendments
495 and organic and inorganic fertilisers. *J. Environ. Manage.* 209, 262-272.
496

497 Atasoy, A., 2005. An investigation on characterization and thermal analysis of the Aughinish
498 red mud. *J. Therm. Anal. Calorim.* 81, 357-361.
499

500 Atasoy, A.D. and Bilgic, B., 2018. Adsorption of copper and zinc ions from aqueous solutions
501 using montmorillonite and bauxite as low-cost adsorbents. *Mine Wat. Environ.* 37, 205-210.
502

503 Balomenos, E., Davris, P., Pontikes, Y. and Panias, D., 2017. Mud2Metal: Lessons learned on
504 the path for complete utilization of bauxite residue through industrial symbiosis. *J. Sustain.*
505 *Metall.* 3, 551-560.
506

507 Bhatnagar, A., Vilar, V.J., Botelho, C.M. and Boaventura, R.A., 2011. A review of the use of
508 red mud as adsorbent for the removal of toxic pollutants from water and wastewater. *Environ.*
509 *Technol.* 32, 231-249.
510

511 Binnemans, K. and Jones, P.T., 2015. Rare earths and the balance problem. *J. Sustain. Metall.*
512 1, 29-38.
513

514 Binnemans, K., Jones, P.T., Blanpain, B., Van Gerven, T. and Pontikes, Y., 2015. Towards
515 zero-waste valorisation of rare-earth-containing industrial process residues: a critical review.
516 *J. Clean. Prod.* 99, 17-38.
517

518 Binnemans, K., Jones, P.T., Müller, T. and Yurramendi, L., 2018. Rare earths and the balance
519 problem: how to deal with changing markets? J. Sustain. Metall. 4, 1-21.
520

521 Blake, G.R., 1965. Bulk Density 1. Methods of soil analysis. Part 1. Physical and mineralogical
522 properties, including statistics of measurement and sampling, (methodsofsoilana), 374-390.
523 Available:
524 <https://dl.sciencesocieties.org/publications/books/tocs/agronomymonogra/methodsofsoilana>
525 [accessed 24.05.2018].
526

527 Borra, C.R., Pontikes, Y., Binnemans, K. and Van Gerven, T., 2015. Leaching of rare earths
528 from bauxite residue (red mud). Minerals Engin. 76, 20-27.
529

530 Bridger, S. and Knowles, M., 2000. A complete method for environmental samples by
531 simultaneous axially viewed ICP-AES following USEPA guidelines. Varian ICP-OES At
532 Work (29). Available: <https://www.agilent.com/cs/library/applications/ICPES-29.pdf>
533 [accessed 24.05.2018].
534

535 Burke, I.T., Peacock, C.L., Lockwood, C.L., Stewart, D.I., Mortimer, R.J., Ward, M.B.,
536 Renforth, P., Gruiz, K. and Mayes, W.M., 2013. Behavior of aluminum, arsenic, and vanadium
537 during the neutralization of red mud leachate by HCl, gypsum, or seawater. Environ. Sci.
538 Technol. 47, 6527-6535.
539

540 Castaldi, P., Silvetti, M., Enzo, S. and Deiana, S., 2011. X-ray diffraction and thermal analysis
541 of bauxite ore-processing waste (red mud) exchanged with arsenate and phosphate. Clays and
542 Clay Min. 59, 189-199.

543
544
545
546
547
548
549
550
551
552
553
554
555
556
557
558
559
560
561
562
563
564
565
566
567

Clohesy, J., 2015. Closure and rehabilitation of Rusal Aughinish BRDA, presented at the Residue Closure and Rehabilitation Workshop. In 10th Alumina Quality Workshop, Perth, Western Australia. Available: (<http://aqw.com.au/2015papers.html>) [accessed 18.04.2018].

Cooling, D.J., 2007. Improving the sustainability of residue management practices-Alcoa World Alumina Australia. Paste and thickened tailings: a guide, 316. Available: <http://citeseerx.ist.psu.edu/viewdoc/download?doi=10.1.1.629.1067&rep=rep1&type=pdf> [accessed 24.05.2018].

Courtney, R. and Harrington, T., 2010. Assessment of plant-available phosphorus in a fine textured sodic substrate. *Ecol. Engin.* 36, 542-547.

Communication from the commission to the European Parliament, the council, the European economic and social committee and the committee of the regions, 2017. Available: <http://eur-lex.europa.eu/legal-content/EN/TXT/PDF/?uri=CELEX:52017DC0490&from=EN> [accessed 26.02.2018].

Cusack, P.B., Healy, M.G., Ryan, P.C., Burke, I.T., O'Donoghue, L.M., Ujaczki, É. and Courtney, R., 2018. Enhancement of bauxite residue as a low-cost adsorbent for phosphorus in aqueous solution, using seawater and gypsum treatments. *J. Clean. Prod.* 179, 217-224.

Dursun, S., Guclu, D., Berktaç, A. and Guner, T. 2008. Removal of chromate from aqueous system by activated red-mud. *Asian J. Chem.* 20, 6473–6478.

568 EU Communities Commission Decision 2000/532/EC, OJ L 226, 06.09.2000; pp. 3–24.
569 Available online: [http://eur-lex.europa.eu/legal-](http://eur-lex.europa.eu/legal-content/EN/TXT/PDF/?uri=CELEX:22002D0009&from=EN)
570 [content/EN/TXT/PDF/?uri=CELEX:22002D0009&from=EN](http://eur-lex.europa.eu/legal-content/EN/TXT/PDF/?uri=CELEX:22002D0009&from=EN) [accessed 27.09.2018].
571

572 EU Communities Council Directive 1999/31/EC on the landfill of waste, OJ L 182, 16.07.1999;
573 pp. 1–19. Available online:[http://eur-lex.europa.eu/legal-](http://eur-lex.europa.eu/legal-content/EN/TXT/PDF/?uri=CELEX:31999L0031&from=EN)
574 [content/EN/TXT/PDF/?uri=CELEX:31999L0031&from=EN](http://eur-lex.europa.eu/legal-content/EN/TXT/PDF/?uri=CELEX:31999L0031&from=EN) [accessed on 27.09.2018].
575

576 European Commission, 2017. Study on the review of the list of critical raw materials. Critical
577 raw materials factsheets. Catalogue number ET-04-15-307-EN-N. Available:
578 [https://publications.europa.eu/en/publication-detail/-/publication/7345e3e8-98fc-11e7-b92d-](https://publications.europa.eu/en/publication-detail/-/publication/7345e3e8-98fc-11e7-b92d-01aa75ed71a1/language-en)
579 [01aa75ed71a1/language-en](https://publications.europa.eu/en/publication-detail/-/publication/7345e3e8-98fc-11e7-b92d-01aa75ed71a1/language-en) [accessed 15.05.2018].
580

581 Evans, K., 2016. The history, challenges, and new developments in the management and use
582 of bauxite residue. *J. Sustain Metall.* 2, 316-331.
583

584 Goloran, J.B., Chen, C.R., Phillips, I.R., Xu, Z.H. and Condrón, L.M., 2013. Selecting a
585 nitrogen availability index for understanding plant nutrient dynamics in rehabilitated bauxite-
586 processing residue sand. *Ecol. Engin.* 58, 228-237.
587

588 Gomes, H.I., Jones, A., Rogerson, M., Burke, I.T. and Mayes, W.M., 2016. Vanadium removal
589 and recovery from bauxite residue leachates by ion exchange. *Environ. Sci. Poll. Res.* 23,
590 23034-23042.
591

592 Grace, M.A., Healy, M.G. and Clifford, E., 2015. Use of industrial by-products and natural
593 media to adsorb nutrients, metals and organic carbon from drinking water. *Sci. Tot. Environ.*
594 518, 491-497.

595

596 Grace, M.A., Clifford, E. and Healy, M.G., 2016. The potential for the use of waste products
597 from a variety of sectors in water treatment processes. *J. Clean. Prod.* 137, 788-802.

598

599 Gräfe, M., Power, G. and Klauber, C., 2011. Bauxite residue issues: III. Alkalinity and
600 associated chemistry. *Hydrometallurgy* 108, 60-79.

601

602 Ha, X.L., Hoang, N.H., Nguyen, T.T.N., Nguyen, T.T., Nguyen, T.H., Dang, V.T. and Nguyen,
603 N.H., 2017, October. Removal of Cd (II) from aqueous solutions using red mud/graphene
604 composite. In *Congrès International de Géotechnique–Ouvrages–Structures (1044-1052)*.
605 Springer, Singapore.

606

607 Han, Y.S., Ji, S., Lee, P.K. and Oh, C., 2017. Bauxite residue neutralization with simultaneous
608 mineral carbonation using atmospheric CO₂. *J. Hazard. Mater.* 326, 87-93.

609

610 Hannachi, Y., Shapovalov, N.A. and Hannachi, A. 2010. Adsorption of nickel from aqueous
611 solution by the use of low-cost adsorbents. *Korean J. Chem. Engin.* 27, 152–158.

612

613 Hertel, T., Blanpain, B. and Pontikes, Y., 2016. A proposal for a 100% use of bauxite residue
614 towards inorganic polymer mortar. *J. Sustain. Metall.* 2, 394-404.

615

616 Higgins, D., Curtin, T., Pawlett, M. and Courtney, R., 2016. The potential for constructed
617 wetlands to treat alkaline bauxite-residue leachate: *Phragmites australis* growth. *Environ. Sci.*
618 *Poll. Res.* 23, 24305-24315.

619

620 Higgins, D., Curtin, T. and Courtney, R., 2017. Effectiveness of a constructed wetland for
621 treating alkaline bauxite residue leachate: a 1-year field study. *Environ. Sci. Poll. Res.* 24,
622 8516-8524.

623

624 IAI, 2015. Bauxite residue management: best practice. [http://www.world-](http://www.world-aluminium.org/media/filer_public/2015/10/15/bauxite_residue_management_-_best_practice_english_oct15edit.pdf)
625 [aluminium.org/media/filer_public/2015/10/15/bauxite_residue_management_-](http://www.world-aluminium.org/media/filer_public/2015/10/15/bauxite_residue_management_-_best_practice_english_oct15edit.pdf)
626 [_best_practice_english_oct15edit.pdf](http://www.world-aluminium.org/media/filer_public/2015/10/15/bauxite_residue_management_-_best_practice_english_oct15edit.pdf). [accessed: 14th October 2017].

627

628 Jones, B.E., Haynes, R.J. and Phillips, I.R., 2012. Addition of an organic amendment and/or
629 residue mud to bauxite residue sand in order to improve its properties as a growth medium. *J.*
630 *Environ. Manage.* 95, 29-38.

631

632 Jowitt, S.M., Werner, T.T., Weng, Z. and Mudd, G.M., 2018. Recycling of the rare Earth
633 elements. *Curr. Opin.Green.Sustain. Chem* 13, 1-7.

634

635 Khaitan, S., Dzombak, D.A., Swallow, P., Schmidt, K., Fu, J. and Lowry, G.V., 2010. Field
636 evaluation of bauxite residue neutralization by carbon dioxide, vegetation, and organic
637 amendments. *J. Environ. Engin.* 136, 1045-1053.

638

639 Kirwan, L.J., Hartshorn, A., McMonagle, J.B., Fleming, L. and Funnell, D., 2013. Chemistry
640 of bauxite residue neutralisation and aspects to implementation. *Int. J. Miner. Process.*, 119,
641 40-50.

642

643 Klauber, C., Gräfe, M. and Power, G., 2011. Bauxite residue issues: II. Options for residue
644 utilization. *Hydrometallurgy* 108, 11-32.

645

646 Kong, X., Guo, Y., Xue, S., Hartley, W., Wu, C., Ye, Y. and Cheng, Q., 2017a. Natural
647 evolution of alkaline characteristics in bauxite residue. *J. Clean. Prod.* 143, 224-230.

648

649 Kong, X., Li, M., Xue, S., Hartley, W., Chen, C., Wu, C., Li, X. and Li, Y., 2017b. Acid
650 transformation of bauxite residue: conversion of its alkaline characteristics. *J. Hazard. Mat.*
651 324, 382-390.

652

653 Kong, X., Tian, T., Xue, S., Hartley, W., Huang, L., Wu, C. and Li, C., 2018. Development of
654 alkaline electrochemical characteristics demonstrates soil formation in bauxite residue
655 undergoing natural rehabilitation. *Land. Degrad. Dev* 29, 58-67.

656

657 Liu, Y. and Naidu, R., 2014. Hidden values in bauxite residue (red mud): recovery of metals.
658 *Waste Manage.* 34, 2662-2673.

659

660 Menzies, N.W., Fulton, I.M., Kopittke, R.A. and Kopittke, P.M., 2009. Fresh water leaching
661 of alkaline bauxite residue after sea water neutralization. *J. Environ. Qual.* 38, 2050-2057.

662

663 McMahon, K. (2017) 'Bauxite Residue Disposal Area Rehabilitation', ISCOBA conference
664 November 2017, Hamburg, 02-05 Oct, Hamburg, Germany. Available:
665 [http://icsoba.org/sites/default/files/2017papers/Bauxite%20Residue%20Papers/BR01%20-](http://icsoba.org/sites/default/files/2017papers/Bauxite%20Residue%20Papers/BR01%20-%20Bauxite%20Residue%20Disposal%20Area%20Rehabilitation.pdf)
666 [%20Bauxite%20Residue%20Disposal%20Area%20Rehabilitation.pdf](http://icsoba.org/sites/default/files/2017papers/Bauxite%20Residue%20Papers/BR01%20-%20Bauxite%20Residue%20Disposal%20Area%20Rehabilitation.pdf) [accessed:
667 21.02.2018].
668
669 Mohapatra, B.K., Mishra, B.K. and Mishra, C.R., 2012. Studies on metal flow from khondalite
670 to bauxite to alumina and rejects from an alumina refinery, India. In Light Metals 2012 (87-
671 91). Springer, Cham.
672
673 Morel, A., Borjon-Piron, Y., Porto, R.L., Brousse, T. and Bélanger, D., 2016. Suitable
674 conditions for the use of vanadium nitride as an electrode for electrochemical capacitor. J.
675 Electrochem. Soc. 163, A1077-A1082.
676
677 Nikbin, I.M., Aliaghazadeh, M., Charkhtab, S. and Fathollahpour, A., 2018. Environmental
678 impacts and mechanical properties of lightweight concrete containing bauxite residue (red
679 mud). J. Clean. Prod. 172, 2683-2694.
680
681 Petrakova, O.V., Panov, A.V., Gorbachev, S.N., Klimentenok, G.N., Perestoronin, A.V.,
682 Vishnyakov, S.E. and Anashkin, V.S., 2015. Improved efficiency of red mud processing
683 through scandium oxide recovery. In Light Metals 2015 (93-96). Springer, Cham.
684
685 Pontikes, Y., Rathossi, C., Nikolopoulos, P., Angelopoulos, G.N., Jayaseelan, D.D. and Lee,
686 W.E., 2009. Effect of firing temperature and atmosphere on sintering of ceramics made from
687 Bayer process bauxite residue. Ceramics Internat. 35, 401-407.

688

689 Pontikes, Y. and Angelopoulos, G.N., 2013. Bauxite residue in cement and cementitious
690 applications: current status and a possible way forward. *Resour. Conserv. Recycl* 73, 53-63.

691

692 Power, G., Gräfe, M. and Klauber, C., 2011. Bauxite residue issues: I. current management,
693 disposal and storage practices. *Hydrometallurgy* 108, 33-45.

694

695 Qin, S., Sun, Y., Li, Y., Wang, J., Zhao, C. and Gao, K., 2015. Coal deposits as promising
696 alternative sources for gallium. *Earth-Science Reviews* 150, 95-101.

697

698 Qin, B. and Schneider, U., 2016. Catalytic use of elemental gallium for carbon–carbon bond
699 formation. *J. Am. Chem. Soc* 138, 13119-13122.

700

701 Ricketts, N.J. and Duyvesteyn, W.P., 2018, March. Scandium recovery from the Nyngan
702 laterite project in NSW. In *TMS Annual Meeting & Exhibition (1539-1543)*. Springer, Cham.

703

704 Santini, T.C. and Fey, M.V., 2013. Spontaneous vegetation encroachment upon bauxite residue
705 (red mud) as an indicator and facilitator of in situ remediation processes. *Environ. Sci. Technol.*
706 47, 12089-12096.

707

708 Tsakiridis, P.E., Agatzini-Leonardou, S. and Oustadakis, P., 2004. Red mud addition in the raw
709 meal for the production of Portland cement clinker. *J. Hazard. Mat.* 116, 103-110.

710

711 Ujaczki, É., Klebercz, O., Feigl, V., Molnár, M., Magyar, Á., Uzinger, N. and Gruiz, K.,
712 2015. Environmental toxicity assessment of the spilled Ajka red mud in soil microcosms for
713 its potential utilisation as soil ameliorant. *Periodica Polytechnica. Chem. Engin.* 59, 253.
714

715 Ujaczki, É., Zimmermann, Y., Gasser, C., Molnár, M., Feigl, V. and Lenz, M., 2017. Red mud
716 as secondary source for critical raw materials–purification of rare earth elements by
717 liquid/liquid extraction. *J. Chem. Technol. Biotech.* 92, 2835-2844.
718

719 Ujaczki, É., Feigl, V., Molnár, M., Cusack, P., Curtin, T., Courtney, R., O'Donoghue, L.,
720 Davris, P., Hugi, C., Evangelou, M.W. and Balomenos, E., 2018. Re-using bauxite residues:
721 benefits beyond (critical raw) material recovery. *J. Chem. Technol. Biotech* 93, 2498-2510.
722

723 United States Geological Survey Website (USGS). Commodity Statistics and Information
724 (2016). Available: <http://minerals.usgs.gov/minerals/pubs/commodity/> [accessed 30.01.2018].
725

726 Wang, S., Ang, H.M. and Tade, M.O., 2008. Novel applications of red mud as coagulant,
727 adsorbent and catalyst for environmentally benign processes. *Chemosphere* 72, 1621-1635.
728

729 Wang, W., Pranolo, Y. and Cheng, C.Y., 2013. Recovery of scandium from synthetic red mud
730 leach solutions by solvent extraction with D2EHPA. *Sep.Purif. Technol* 108, 96-102.
731

732 Wang, X., Zhang, Y., Lv, F., An, Q., Lu, R., Hu, P. and Jiang, S., 2015. Removal of alkali in
733 the red mud by SO₂ and simulated flue gas under mild conditions. *Environ. Prog. Sustain.*
734 *Ener.* 34, 81-87.
735

736 Weng, Z., Jowitt, S.M., Mudd, G.M. and Haque, N., 2015. A detailed assessment of global rare
737 earth element resources: opportunities and challenges. *Econ. Geol.* 110, 1925-1952.
738

739 Xu, C., Kynický, J., Smith, M.P., Kopriva, A., Brtnický, M., Urubek, T., Yang, Y., Zhao, Z.,
740 He, C. and Song, W., 2017. Origin of heavy rare earth mineralization in South China. *Nature*
741 *Comm.* 8, 14598.
742

743 Xue, S., Kong, X., Zhu, F., Hartley, W., Li, X. and Li, Y., 2016. Proposal for management and
744 alkalinity transformation of bauxite residue in China. *Environ. Sci. Poll. Res.* 23, 12822-12834.
745

746 Xue, S., Li, M., Jiang, J., Millar, G.J., Li, C. and Kong, X., 2018. Phosphogypsum
747 stabilization of bauxite residue: conversion of its alkaline characteristics. *J. Environ. Sci.*
748 <https://doi.org/10.1016/j.jes.2018.05.016>
749

750 Zhu, F., Liao, J., Xue, S., Hartley, W., Zou, Q. and Wu, H., 2016. Evaluation of aggregate
751 microstructures following natural regeneration in bauxite residue as characterized by
752 synchrotron-based X-ray micro-computed tomography. *Sci. Tot. Environ.* 573, 155-163.
753

754 Zhu, F., Xue, S., Hartley, W., Huang, L., Wu, C. and Li, X., 2016. Novel predictors of soil
755 genesis following natural weathering processes of bauxite residues. *Environ. Sci. Poll. Res.* 23,
756 2856-2863.
757

758 Zhu, F., Cheng, Q., Xue, S., Li, C., Hartley, W., Wu, C. and Tian, T., 2018. Influence of natural
759 regeneration on fractal features of residue microaggregates in bauxite residue disposal areas.
760 *Land Degrad. Dev.* 29, 138-149.

761 **Table 1** Sample information regarding the year of production for each of the bauxite residue samples
762 over a twelve-year period. The sample code for each bauxite residue sample is also included in the
763 table.

Sample Code	Sample Description	Year of Disposal
BR 12	Bauxite Residue	2004
BR 11	Bauxite Residue	2005
BR 10	Bauxite Residue	2006
BR 9	Bauxite Residue	2007
BR 8	Bauxite Residue	2008
BR 7	Bauxite Residue	2009
BR 6	Bauxite Residue	2010
BR 5	Bauxite Residue	2011
BR 4	Bauxite Residue	2012
BR 3	Bauxite Residue	2013
BR 2	Bauxite Residue	2014
BR 1	Bauxite Residue	2015

764
765
766
767
768
769
770
771
772
773
774
775

776 **Table 2** Physico-chemical composition of the bauxite residue mud over a twelve-year storage period,
 777 inclusive of pH, EC, moisture content, bulk density and particle size distribution.

Sample	pH	EC (mS cm ⁻¹)	Moisture content (%)	Bulk density (g cm ⁻³)	d ₁₀ (μm) ^a	d ₅₀ (μm) ^b	d ₉₀ (μm) ^c
BR 12	11.6 ± 0.02	1.0 ± 0.01	26.8 ± 0.7	1.4 ± 0.04	0.7 ± 0.1	2.6 ± 0.1	7.0 ± 1.2
BR 11	10.8 ± 0.1	0.4 ± 0.02	28.2 ± 0.7	1.3 ± 0.03	0.9 ± 0.1	3.5 ± 0.5	9.6 ± 0.5
BR 10	12.0 ± 0.02	3.3 ± 0.2	26.8 ± 0.1	1.4 ± 0.1	1.4 ± 0.1	4.0 ± 0.3	12.3 ± 1.6
BR 9	10.0 ± 0.1	0.4 ± 0.01	24.3 ± 0.3	1.1 ± 0.1	1.0 ± 0.1	4.3 ± 0.4	12.4 ± 1.0
BR 8	11.4 ± 0.1	1.0 ± 0.1	27.2 ± 0.3	1.4 ± 0.1	0.8 ± 0.1	2.6 ± 0.1	6.8 ± 0.2
BR 7	10.4 ± 0.02	0.5 ± 0.01	22.3 ± 0.6	1.4 ± 0.04	0.9 ± 0.2	3.2 ± 0.5	12.7 ± 2.7
BR 6	10.7 ± 0.03	0.5 ± 0.03	25.8 ± 1.0	1.3 ± 0.04	0.7 ± 0.1	2.6 ± 0.01	6.7 ± 0.2
BR 5	10.3 ± 0.1	0.4 ± 0.03	22.0 ± 0.5	1.2 ± 0.1	0.6 ± 0.01	2.4 ± 0.04	7.9 ± 1.1
BR 4	11.5 ± 0.1	0.9 ± 0.02	31.1 ± 0.5	1.3 ± 0.1	1.2 ± 0.1	3.8 ± 0.6	12.70 ± 2.3
BR 3	10.6 ± 0.02	0.5 ± 0.01	23.8 ± 0.3	1.3 ± 0.03	0.8 ± 0.2	2.6 ± 0.3	8.3 ± 1.6
BR 2	11.2 ± 0.01	0.9 ± 0.02	28.1 ± 1.9	1.3 ± 0.1	1.1 ± 0.02	3.2 ± 0.02	9.7 ± 0.9
BR 1	10.3 ± 0.1	0.7 ± 0.03	25.0 ± 2.7	1.5 ± 0.02	0.5 ± 0.01	2.2 ± 0.1	6.7 ± 0.6

778 ^ad₁₀ (μm) = the size of particles at 10% of the total particle distribution.

779 ^bd₅₀ (μm) = the median; the size of particles at 50% of the total particle distribution.

780 ^cd₉₀ (μm) = the size of particles at 90% of the total particle distribution.

781

782

783

784

785

786

787

788

789

790

791

792

793 **Table 3** Main mineralogical composition (%) of the bauxite residue samples taken from the BRDA
 794 ranging from one to twelve years old, as determined by XRF.

Code	Al ₂ O ₃	Fe ₂ O	SiO ₂	TiO ₂	CaO
BR 11	17.0±0.61	42.0±1.20	9.82±0.32	9.41±0.34	6.03±0.79
BR 10	17.1±0.4	41.5±0.96	10.2±0.56	9.52±0.6	6.03±0.49
BR 9	17.8±0.73	40.1±1.40	10.9±0.47	8.97±0.51	6.04±0.4
BR 8	16.8±0.58	41.8±1.40	9.89±0.39	9.41±0.61	5.97±0.49
BR 7	14.8±1.5	47.5±2.0	7.20±1.0	10.3±0.95	6.1±1.0
BR 6	16.2±0.54	45.9±2.10	8.0±0.57	9.54±0.78	5.70±0.66
BR 5	16.2±0.66	44.4±1.30	9.35±0.60	8.62±0.71	5.75±0.53
BR 4	16.5±0.65	43.3±1.20	9.38±0.53	8.91±0.53	6.21±0.35
BR 3	15.8±0.45	44.3±1.90	8.85±0.47	9.18±0.62	6.34±0.35
BR 2	16.0±0.71	46.6±1.80	8.95±0.70	8.21±0.38	5.0±0.40
BR 1	16.2±0.6	46.8±1.61	8.76±0.48	8.33±0.56	4.69±0.43

795

796

797

798

799

800

801

802

803

804

805

806

807

808

809

810 **Table 4** CRM composition (in mg kg⁻¹) of the bauxite residue samples, taken from the BRDA, as detected on ICP-OES following aqua regia digestion.

Element	BR 12	BR 11	BR 10	BR 9	BR 8	BR 7	BR 6	BR 5	BR 4	BR 3	BR 2
Dy	3.6 ± 0.02	5.4 ± 0.01	7.19 ± 0.01	5.39 ± 0.001	5.4 ± 0.04	5.39 ± 0.01	5.4 ± 0.01	5.38 ± 0.02	4.51 ± 1.3	7.2 ± 0.002	5.4 ± 0.02
Er	4.8 ± 0.5	5.4 ± 0.01	5.7 ± 0.5	4.94 ± 0.6	5.4 ± 0.04	5.39 ± 0.01	4.49 ± 0.01	5.38 ± 0.01	4.05 ± 0.6	5.4 ± 0.001	5.4 ± 0.02
Lu	8.39 ± 0.5	7.8 ± 0.5	8.09 ± 0.01	7.49 ± 0.5	8.1 ± 0.05	7.63 ± 0.6	8.1 ± 0.02	8.37 ± 0.5	7.66 ± 0.7	8.1 ± 0.002	8.09 ± 0.03
Y	35.6 ± 3.2	39.8 ± 1.2	44.4 ± 1.5	41.9 ± 1.5	42 ± 0.4	39.5 ± 0.04	33.4 ± 0.4	41 ± 2.0	36.9 ± 1.4	47.4 ± 1.2	39.3 ± 0.5
Yb	8.39 ± 0.6	8.8 ± 0.3	9.39 ± 0.3	8.79 ± 0.7	9.4 ± 0.3	8.68 ± 0.4	8.2 ± 0.4	8.97 ± 0.9	8.11 ± 0.4	9.6 ± 0.002	8.71 ± 0.4
Ce	126 ± 10.1	126 ± 3.5	156 ± 2.2	136 ± 7.6	157 ± 2.2	128 ± 3.3	146 ± 6.7	200 ± 8.4	102 ± 3.5	147 ± 4.2	139 ± 6.8
Eu	2.40 ± 0.01	2.40 ± 0.01	2.40 ± 0.005	2.40 ± 0.01	2.40 ± 0.02	2.39 ± 0.003	2.40 ± 0.01	3.59 ± 0.01	2.40 ± 0.01	2.40 ± 0.001	2.40 ± 0.005
Gd	6.75 ± 0.6	6.60 ± 0.5	7.64 ± 0.6	7.63 ± 0.6	9.30 ± 0.6	7.18 ± 1.3	6.75 ± 0.6	8.98 ± 0.02	5.41 ± 0.02	9 ± 0.002	6.73 ± 0.6
La	91.3 ± 8.6	88.2 ± 3.2	108 ± 2.3	94.1 ± 2.7	106.4 ± 1.0	89.2 ± 0.9	104 ± 3.5	134 ± 4.4	68.8 ± 4.0	98.2 ± 2.1	91 ± 2.4
Nd	80.1 ± 7.4	77.2 ± 5.3	93.9 ± 6.5	84.7 ± 1.3	98 ± 5.3	85.6 ± 8.6	88.9 ± 8.6	118 ± 4.4	64.6 ± 4.0	93 ± 2.2	94.3 ± 11.3
Pr	41.1 ± 3.5	42.9 ± 4.2	47.7 ± 3.3	42.5 ± 3.1	50.1 ± 1.6	40.8 ± 1.9	45 ± 2.7	56.2 ± 5.3	34.7 ± 3.3	45 ± 0.9	42.3 ± 1.1
Sc	50.2 ± 4.1	50.4 ± 1.6	60.2 ± 2.2	56.1 ± 2.7	54.2 ± 0.9	55.7 ± 1.3	45.4 ± 0.2	56 ± 4.2	42.9 ± 2.3	49 ± 1.3	45.6 ± 4.3
Sm	19.3 ± 0.7	20.7 ± 1.8	21 ± 2.2	21.6 ± 0.9	21.6 ± 0.8	18.4 ± 1.9	21.6 ± 0.9	25.1 ± 0.05	18 ± 1.2	21 ± 1.0	20.3 ± 2.0

Co	8.69 ± 0.5	7.64 ± 0.6	7.79 ± 0.5	6.73 ± 0.6	8.10 ± 0.05	7.63 ± 0.6	6.6 ± 0.5	8.67 ± 0.5	7.21 ± 0.02	8.4 ± 0.5	7.49 ± 0.6
Ga	107 ± 8.5	112 ± 2.3	102 ± 0.7	114 ± 5.2	98.6 ± 0.2	113 ± 3.8	106 ± 2.7	114 ± 5.1	99.5 ± 1.8	114 ± 1.9	94.4 ± 2.7
In	30.1 ± 1.8	34.6 ± 0.7	31.5 ± 1.5	32.1 ± 2.7	36.9 ± 0.9	30.5 ± 1.3	29.2 ± 2	33.6 ± 0.7	28.4 ± 0.7	34.5 ± 7.2	36.4 ± 4.3
Mo	3.14 ± 0.6	4.49 ± 0.01	4.04 ± 0.6	4.95 ± 0.6	4.48 ± 0.004	4.95 ± 0.6	4.49 ± 0.01	4.48 ± 0.01	4.94 ± 1.9	4.8 ± 0.5	4.48 ± 0.01
V	593 ± 60.6	419 ± 8.2	596 ± 19.8	439 ± 41.1	491 ± 20.3	445 ± 41.2	484 ± 48.2	600 ± 24.3	401 ± 41.2	571 ± 13.3	573 ± 41.1

811

812 **Table 5** Associated financial value of economically interesting elements in the bauxite residue (average
 813 over a twelve-year period, n = 11).

Element	Average aqua regia extracted content (mg kg ⁻¹)	Price* (US \$ t ⁻¹)	Economic value of the bauxite residue in this study*** (US \$ t ⁻¹)
Ga	107±7.3	400,000	42.73
Sc	51.4±5.4	4,600,000	236.44
In	32.5±2.9	240,000	7.81
V	510±77.8	6,889	3.51
Nd	89.0±13.6	39,500	3.51
Dy	5.48±1.0	184,500	1.01
Pr	44.4±5.6	5,500**	0.24
Y	40.1±3.9	35,500	1.42
Ce	142±24.9	2,000	0.28
Sm	20.8±1.9	12,500**	0.26
Co	7.72±0.7	26,444	0.20
La	97.5±16.3	2,000	0.19
Eu	2.51±0.4	66,000	0.16
Yb	8.82±0.5	5,500**	0.04
Lu	7.99±0.3	5,500**	0.04
Gd	7.45±1.2	5,500**	0.04
Mo	4.48±0.5	14,500	0.06
Er	5.12±0.5	5,500**	0.03

814 *Values from USGS (2016)

815 **Average value for mischmetals of REE/expected higher individual prices

816 *** Economic value of the bauxite residue in this study, determined using current price (US \$ t⁻¹) and the average
 817 content in the bauxite residue studied.

818

819

820

821

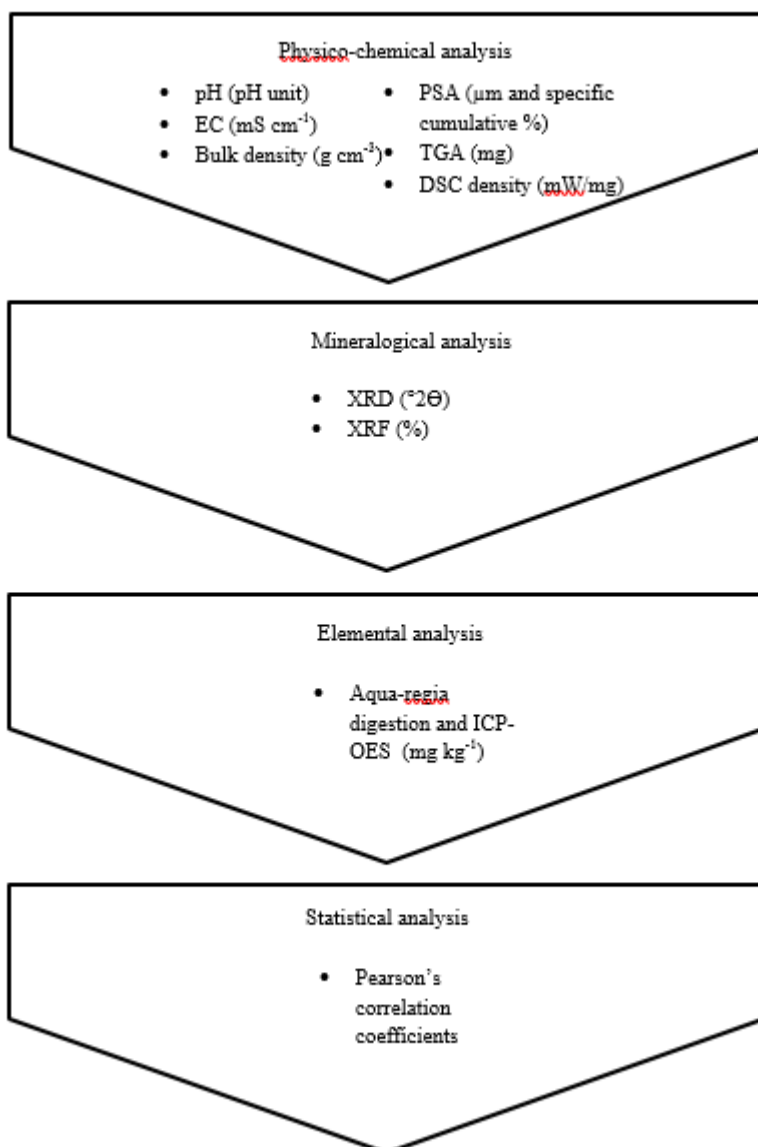
822

823

824

825

826



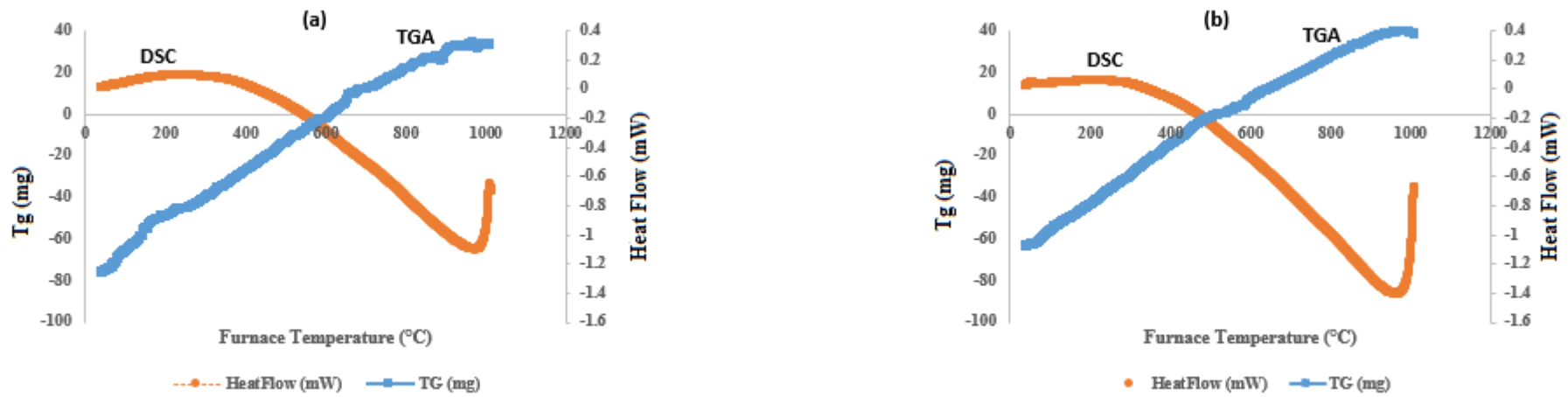
827

828

829 **Figure 1** Flow chart illustrating the experimental analysis carried out on the bauxite residue samples
 830 obtained. Once obtained from the BRDA, the bauxite residue was analysed for its main physico-
 831 chemical analysis (pH, EC, bulk density, PSA, TGA and DSC), mineralogical analysis (XRD and
 832 XRF), and elemental analysis (measure using ICP-OES following aqua-regia digestion). Once all
 833 data was obtained, statistical analysis was carried out using Pearson's correlation coefficients.

834

835



836 **Figure 2** TGA (descending) / DSC (ascending) curve obtained for bauxite residue (a) BR12 (2004) and (b) BR2 (2014). Remaining TGA / DSC graphs
 837 found in Figure S4. The TGA curves showed weight loss between 300 and 975 °C for all the bauxite residues examined.

